National and Global Petroleum Assessment

Assessment of Undiscovered Conventional Oil and Gas Resources of China, 2020

*U*sing a geology-based assessment methodology, the U.S. Geological Survey estimated undiscovered, technically recoverable mean resources of 13.4 billion barrels of oil and 244.4 trillion cubic feet of gas in nine geologic provinces of China.

Introduction

The U.S. Geological Survey (USGS) quantitatively assessed the potential for undiscovered, technically recoverable conventional oil and gas resources in nine geologic provinces of China (fig. 1). This assessment includes the Tarim Basin, Junggar Basin, Turpan Basin, Qaidam Basin, Sichuan Basin, Ordos Basin, Bohaiwan Basin, Songliao Basin, and the East China Sea Basin Provinces. Within these 9 provinces, 16 geologic assessment units (AUs) were defined, and each AU was assessed for undiscovered conventional oil, gas, and natural-gas liquids.

China contains a mosaic of cratonic terranes, remnants of oceanic crust, orogenic belts, suture zones, accretionary complexes, island-arc assemblages, and regional faults that record a complex history of terrane accretion and orogeny along the southern and eastern margins of Eurasia (Liu and others, 2013; Zheng and others, 2013; Zhao and others, 2014; Han and Zhao, 2018; Zhou and others, 2018). Beginning in the Paleozoic, several cratonic blocks separated diachronously from the northern margin of Gondwana and translated north across the Tethys Ocean as oceanic crust was subducted; these terranes eventually collided and accreted, knitting together a collage of tectonic elements. Major cratonic terranes that accreted to Eurasia included the Tarim Basin, Ordos Basin, and Sichuan Basin Provinces. In contrast, the basement of the Junggar, Turpan, Qaidam, and Songliao Basin Provinces are interpreted as fragments of oceanic crust that were not subducted, but rather were incorporated into orogenic belts (Mao and others, 2016; Han and Zhao, 2018). As accretion proceeded, the margins of the cratonic and oceanic fragments became sites of fold and thrust belts, suture zones, faults, and an amalgamation of island-arc and accretionary complexes; several of the terranes developed foreland basins. By the Permian, compressive deformation developed sufficient tectonic topography to isolate several of the basins from marine waters. This topographic relief led to hydraulically closed basins (Garcia-Castellanos, 2006; Marenssi and others, 2020), characterized by the development of extensive, basinwide lacustrine systems. The Junggar and Turpan Basin Provinces developed lacustrine systems by compressive deformation along the margins in the Permian, and lacustrine systems formed following compressional deformation in the Sichuan, Ordos, Tarim, and Qaidam Basin Provinces. In contrast, horst and graben systems along the eastern margin of Eurasia were formed by widespread back-arc extension related to changing motions of the Pacific plate. Extensive lacustrine systems formed within grabens in the Songliao, Bohaiwan, and East China Sea Basin Provinces (Li and others, 2012; Liang and Wang, 2019; Yang and others, 2020).

Petroleum source rocks within these nine provinces reflect the long and complex tectonic history (Jiang and others, 2016). As the cratonic blocks separated from Gondwana and traversed the Tethyan realm in the early Paleozoic, organic-rich marine sediments were deposited in basinal positions mainly associated with passive margin carbonate platforms, such as in the Tarim, Sichuan, and Ordos Basin Provinces (Yang and others, 2005). In the late Paleozoic, subsequent terrane collisions led to the development of marginal fold belts and associated foreland basins. Potential source rocks in the upper Paleozoic foreland basins are dominated by marginal marine to nonmarine, coal-bearing gas-prone sequences. Beginning in the Permian, along with the compressional formation of hydraulically closed basins, climatic conditions were appropriate to form extensive lacustrine systems with viable lacustrine source rocks, which are well known in the basins of China (Jiang and others, 2016).

The Sichuan Basin Province, which resides in the western part of the South China terrane, provides an example of the evolution of the tectonic control on the development of petroleum source rocks (Shi and others, 2016; Mu and others, 2019). The cratonic terrane of the Sichuan Basin Province was rimmed by passive margins as the terrane

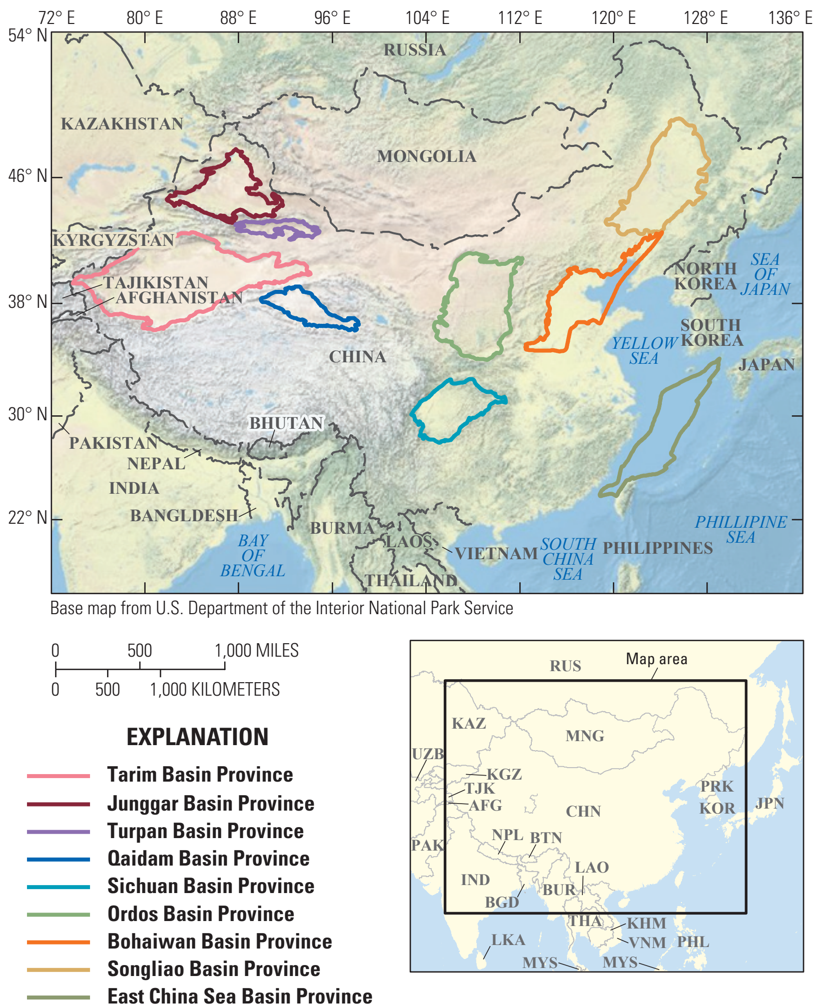

Figure 1. Map showing the location of nine geologic provinces of China assessed in this study.

moved north from Gondwana, which led to the deposition of widespread organic-rich marine source rocks. As the South China terrane impinged on the Eurasia margin, a foreland basin was formed in the Sichuan Basin Province and was the depositional site for marine, marginal marine, and coal-bearing sequences. In the Late Triassic, as the South China terrane collided with the North China and Songpan Ganzi terranes, compressional deformation resulted in topography, a hydraulically closed basin, and the development of an extensive basinwide lacustrine system. A similar temporal development of marine to nonmarine source rocks is interpreted for the Tarim Basin Province (Jin and others, 2008; Wang and others, 2019). In contrast, because the Junggar Basin Province is floored by upper Paleozoic oceanic crust, there is no lower Paleozoic section. Permian deformation isolated the Junggar Basin from marine waters, and the principal petroleum source rocks developed within a lacustrine depositional system. The Turpan and Qaidam Basin Provinces illustrate a similar tectonic development of lacustrine source-rock conditions.

The Bohaiwan Basin Province is an example of the development of lacustrine conditions in an extensional system resulting from complex motion during the subduction of the Pacific plate (Allen and others, 1998). Extension resulted in a regional system of horsts and grabens, which were isolated from marine waters, and many of the grabens developed lacustrine depositional systems (Feng and others, 2016). This process also led to lacustrine systems being formed in the Songliao and East China Sea Basin Provinces (Ge and others, 2012; Wang and others, 2016; Liang and Wang, 2019; Yang and others, 2020). Key assessment input data are summarized in table 1.

Table 1. Key input data for 16 conventional assessment units in China.

[Shading indicates not applicable. AU, assessment unit; MMBO, million barrels of oil; BCFG, billion cubic feet of gas]

Assessment input data—Conventional AUs	Tarim Mesozoic–Cenozoic Reservoirs AU				Tarim Paleozoic Reservoirs AU			
	Minimum	Median	Maximum	Calculated mean	Minimum	Median	Maximum	Calculated mean
Number of oil fields	1	30	90	31.9	1	100	200	102.5
Number of gas fields	1	50	150	53.2	1	250	500	256.1
Size of oil fields (MMBO)	5	8	200	12.2	5	8	3,500	37.3
Size of gas fields (BCFG)	30	60	20,000	260.1	30	60	20,000	260.1
AU probability	1.0				1.0			
Assessment input data—Conventional AUs	**Junggar Upper Paleozoic–Cenozoic Reservoirs AU**				**Turpan Mesozoic–Cenozoic Reservoirs AU**			
	Minimum	Median	Maximum	Calculated mean	Minimum	Median	Maximum	Calculated mean
Number of oil fields	1	45	90	46.1	1	12	25	12.3
Number of gas fields	1	80	160	82.0	1	12	25	12.3
Size of oil fields (MMBO)	5	10	700	21.7	5	8	200	12.2
Size of gas fields (BCFG)	30	72	12,000	230.8	30	60	3,500	122.0
AU probability	1.0				1.0			
Assessment input data—Conventional AUs	**Qaidam Mesozoic–Cenozoic Reservoirs AU**				**Sichuan Southeast Fold Belt Reservoirs AU**			
	Minimum	Median	Maximum	Calculated mean	Minimum	Median	Maximum	Calculated mean
Number of oil fields	1	40	80	41.0				
Number of gas fields	1	40	80	41.0	1	300	600	307.3
Size of oil fields (MMBO)	5	10	200	14.8				
Size of gas fields (BCFG)	30	72	5,000	160.2	6	36	10,000	161.9
AU probability	1.0				1.0			
Assessment input data—Conventional AUs	**Sichuan Foreland Basin Reservoirs AU**				**Sichuan Central Uplift Reservoirs AU**			
	Minimum	Median	Maximum	Calculated mean	Minimum	Median	Maximum	Calculated mean
Number of oil fields					1	4	8	4.1
Number of gas fields	1	150	300	153.7	1	8	16	8.2
Size of oil fields (MMBO)					1	2	20	2.6
Size of gas fields (BCFG)	6	36	3,000	92.1	6	12	100	14.8
AU probability	1.0				1.0			
Assessment input data—Conventional AUs	**Ordos Lower Paleozoic Conventional Reservoirs AU**				**Ordos Western Deformed Belt Reservoirs AU**			
	Minimum	Median	Maximum	Calculated mean	Minimum	Median	Maximum	Calculated mean
Number of oil fields					1	10	30	10.6
Number of gas fields	1	50	150	53.2	1	30	90	31.9
Size of oil fields (MMBO)					5	8	200	12.2
Size of gas fields (BCFG)	30	48	6,000	123.3	30	72	10,000	212.6
AU probability	1.0				0.9			
Assessment input data—Conventional AUs	**Ordos Mesozoic Sandstone Reservoirs AU**				**Bohaiwan Cenozoic Reservoirs AU**			
	Minimum	Median	Maximum	Calculated mean	Minimum	Median	Maximum	Calculated mean
Number of oil fields	1	40	80	41.0	1	500	1,000	512.2
Number of gas fields					1	70	210	74.4
Size of oil fields (MMBO)	5	8	400	14.8	1	2	600	8.2
Size of gas fields (BCFG)					6	24	2,500	66.0
AU probability	1.0				1.0			
Assessment input data—Conventional AUs	**Bohaiwan Mid-Proterozoic–Paleozoic Reservoirs AU**				**Songliao Syn-Rift Sourced Reservoirs AU**			
	Minimum	Median	Maximum	Calculated mean	Minimum	Median	Maximum	Calculated mean
Number of oil fields	1	150	450	159.5	1	10	20	10.3
Number of gas fields	1	50	150	53.2	1	50	100	51.2
Size of oil fields (MMBO)	1	2	40	3.0	5	8	200	12.2
Size of gas fields (BCFG)	6	24	3,000	71.5	30	72	7,000	182.7
AU probability	1.0				1.0			
Assessment input data—Conventional AUs	**Songliao Post-Rift Sourced Reservoirs AU**				**East China Sea Reservoirs AU**			
	Minimum	Median	Maximum	Calculated mean	Minimum	Median	Maximum	Calculated mean
Number of oil fields	1	80	160	82.0	1	30	90	32.0
Number of gas fields	1	10	20	10.3	1	80	240	85.1
Size of oil fields (MMBO)	5	8	300	13.6	5	10	1,000	24.9
Size of gas fields (BCFG)	30	72	4,000	147.7	30	72	12,000	230.8
AU Probability	1.0				1.0			

Undiscovered Resources Summary

The USGS quantitatively assessed undiscovered oil, gas, and natural gas liquids resources within nine geologic provinces of China (table 2). The fully risked mean totals are 13,400 million barrels of oil (MMBO) or 13.4 billion barrels of oil, with a F95–F5 fractile range from 7,022 to 22,267 MMBO; 244,436 billion cubic feet of gas (BCFG), or 244.4 trillion cubic feet, with an F95–F5 range from 122,343 to 412,088 BCFG; and 3,775 million barrels of natural gas liquids (MMBNGL), or 3.8 billion barrels of natural gas liquids, with an F95–F5 range from 1,819 to 6,561 MMBNGL. Assessment results were published previously for the Pearl River Mouth Basin, Beibuwan Basin, Qiongdongnan Basin, and Taixinan Basin Provinces (Schenk and others, 2020).

Table 2. Results for 16 conventional assessment units in China.

[Results shown are fully risked estimates. F95 represents a 95-percent chance of at least the amount tabulated; other fractiles are defined similarly. Shading indicates not applicable. MMBO, million barrels of oil; BCFG, billion cubic feet of gas; NGL, natural gas liquids; MMBNGL, million barrels of natural gas liquids]

Total petroleum system and assessment units (AUs)	AU probability	Accumulation type	Total undiscovered resources											
			Oil (MMBO)				Gas (BCFG)				NGL (MMBNGL)			
			F95	F50	F5	Mean	F95	F50	F5	Mean	F95	F50	F5	Mean
Mesozoic Composite Total Petroleum System, Tarim Basin Province														
Tarim Mesozoic–Cenozoic Reservoirs AU	1.0	Oil	181	361	687	388	380	758	1,441	815	12	24	46	26
		Gas					4,318	12,037	29,875	13,925	156	433	1,075	501
Lower Paleozoic Composite Total Petroleum System, Tarim Basin Province														
Tarim Paleozoic Reservoirs AU	1.0	Oil	1,680	3,505	7,013	3,820	3,862	8,064	16,123	8,787	89	185	371	202
		Gas					37,067	64,208	103,939	66,508	1,001	1,731	2,807	1,796
Paleozoic–Mesozoic Composite Total Petroleum System, Junggar Basin Province														
Junggar Upper Paleozoic–Cenozoic Reservoirs AU	1.0	Oil	525	947	1,657	1,000	469	852	1,498	900	6	10	18	11
		Gas					9,641	17,877	31,791	18,949	115	214	383	227
Paleozoic–Mesozoic Composite Total Petroleum System, Turpan Basin Province														
Turpan Mesozoic–Cenozoic Reservoirs AU	1.0	Oil	77	139	262	150	77	139	263	150	2	3	6	3
		Gas					612	1,307	3,101	1,507	15	33	78	38
Mesozoic–Cenozoic Composite Total Petroleum System, Qaidam Basin Province														
Qaidam Mesozoic–Cenozoic Reservoirs AU	1.0	Oil	368	589	906	606	587	941	1,451	970	1	1	2	1
		Gas					3,350	6,170	11,011	6,547	12	22	39	23
Paleozoic–Mesozoic Composite Total Petroleum System, Sichuan Basin Province														
Sichuan Southeast Fold Belt Reservoirs AU	1.0	Gas					29,376	48,300	75,259	49,808	41	72	118	75
Sichuan Foreland Basin Reservoirs AU	1.0	Gas					8,500	13,744	21,184	14,142	16	26	42	27
Sichuan Central Uplift Reservoirs AU	1.0	Oil	5	10	19	10	8	15	28	16	0	0	0	0
		Gas					70	116	191	122	1	2	3	2
Paleozoic Composite Total Petroleum System, Ordos Basin Province														
Ordos Lower Paleozoic Conventional Reservoirs AU	1.0	Gas					2,571	5,960	12,647	6,558	2	5	12	6
Ordos Western Deformed Belt Reservoirs AU	0.9	Oil	0	110	246	117	0	22	50	23	0	0	0	0
		Gas					0	5,457	13,928	6,097	0	5	13	5
Cenozoic Composite Total Petroleum System, Ordos Basin Province														
Ordos Mesozoic Sandstone Reservoirs AU	1.0	Oil	334	576	976	605	65	115	199	121	0	0	0	0
Cenozoic Composite Total Petroleum System, Bohaiwan Basin Province														
Bohaiwan Cenozoic Reservoirs AU	1.0	Oil	2,576	4,093	6,234	4,203	2,557	4,086	6,260	4,203	20	33	50	34
		Gas					2,055	4,550	8,934	4,896	56	123	241	132
Bohaiwan Mid-Proterozoic–Paleozoic Reservoirs AU	1.0	Oil	241	444	798	471	216	399	720	424	5	8	15	9
		Gas					1,456	3,472	7,309	3,802	34	80	168	87
Songliao Syn-Rift Composite Total Petroleum System, Songliao Basin Province														
Songliao Syn-Rift Sourced Reservoirs AU	1.0	Oil	64	114	222	125	166	297	577	324	1	2	4	2
		Gas					4,704	8,798	15,880	9,350	42	79	144	84
Songliao Post-Rift Sourced Reservoirs AU	1.0	Oil	682	1,082	1,661	1,114	403	648	1,008	669	1	1	2	1
		Gas					583	1,293	3,228	1,514	12	27	68	32
Mesozoic–Cenozoic Composite Total Petroleum System, East China Sea Basin Province														
East China Sea Reservoirs AU	1.0	Oil	289	703	1,586	791	1,331	3,234	7,301	3,640	21	52	117	58
		Gas					7,919	18,120	36,892	19,669	158	363	739	393
Total undiscovered conventional resources			**7,022**	**12,673**	**22,267**	**13,400**	**122,343**	**230,979**	**412,088**	**244,436**	**1,819**	**3,534**	**6,561**	**3,775**

References Cited

Allen, M.B., Macdonald, D.I.M., Xun, Z., Vincent, S.J., and Bronet-Menzies, C., 1998, Transtensional deformation in the evolution of the Bohai Basin, northern China, *in* Holdsworth, R.E., Strachan, R.S., and Dewey, J.F., eds., Continental transpressional and transtensional tectonics: The Geological Society of London Special Publication 135, p. 215–229.

Feng, Y., Jiang, S., Hu, S., Li, S., Lin, C., and Xie, X., 2016, Sequence stratigraphy and importance of syndepositional structural slope-break for architecture of Paleogene syn-rift lacustrine strata, Bohai Bay Basin, China: Marine and Petroleum Geology, v. 69, p. 183–204.

Garcia-Castellanos, D., 2006, Long-term evolution of tectonic lakes—Climatic controls on the development of internally drained basins, *in* Willett, S.D., Hovius, N., Brandon, M.T., and Fisher, D.M., eds., Tectonics, climate, and landscape evolution: Geological Society of America Special Publication 398, p. 283–294. [Also available at https://doi.org/10.1130/2006.2398(17).]

Ge, R., Zhang, Q., Wang, L., Chen, J., Xie, G., and Wang, X., 2012, Late Mesozoic rift evolution and crustal extension in the central Songliao Basin, northeastern China—Constraints from cross-section restoration and implications for lithospheric thinning: International Geology Review, v. 54, no. 2, p. 183–207. [Also available at https://doi.org/10.1080/00206814.2010.511900.]

Han, Y., and Zhao, G., 2018, Final amalgamation of the Tianshan and Junggar orogenic collage in the southwestern Central Asian Orogenic Belt—Constraints on the closure of the Paleo-Asian ocean: Earth-Science Reviews, v. 186, p. 129–152. [Also available at https://doi.org/10.1016/j.earscirev.2017.09.012.]

Jiang, S., Xu, Z., Feng, Y., Zhang, J., Cai, D., Chen, L., Wu, Y., Zhou, D., Bao, S., and Long, S., 2016, Geologic characteristics of hydrocarbon-bearing marine, transitional and lacustrine shales in China: Journal of Asian Earth Sciences, v. 115, p. 404–418. [Also available at https://doi.org/10.1016/j.jseaes.2015.10.016.]

Jin, Z., Yang, M., Lu, X., Sun, D., Tang, X., Peng, G., and Lei, G., 2008, The tectonics and petroleum system of the Qiultagh fold and thrust belt, northern Tarim Basin, NW China: Marine and Petroleum Geology, v. 25, no. 8, p. 767–777. [Also available at https://doi.org/10.1016/j.marpetgeo.2008.01.011.]

Li, S., Zhao, G., Dai, L., Liu, X., Zhou, L., Santosh, M., and Suo, Y., 2012, Mesozoic basins in eastern China and their bearing on the deconstruction of the North China craton: Journal of Asian Earth Sciences, v. 47, p. 64–79. [Also available at https://doi.org/10.1016/j.jseaes.2011.06.008.]

Liang, J., and Wang, H., 2019, Cenozoic tectonic evolution of the East China Sea Shelf Basin and its coupling relationships with Pacific plate subduction: Journal of Asian Earth Sciences, v. 171, p. 376–387. [Also available at https://doi.org/10.1016/j.jseaes.2018.08.030.]

Liu, S., Su, S., and Zhang, G., 2013, Early Mesozoic basin development in North China—Indications of cratonic deformation: Journal of Asian Earth Sciences, v. 62, p. 221–236. [Also available at https://doi.org/10.1016/j.jseaes.2012.09.011.]

Mao, L., Xiao, A., Zhang, H., Wu, Z., Wang, L., Shen, Y., and Wu, L., 2016, Structural deformation patterns within the NW Qaidam Basin in the Cenozoic era and its tectonic implications: Tectonophysics 687, p. 78–93. [Also available at https://doi.org/10.1016/j.tecto.2016.09.008.]

Marenssi, S.A., Limarino, C.O., Schencman, L.J., and Ciccioli, P.I., 2020, Tectonic and geomorphic controls on the lacustrine deposits of the Neogene Vinchina Basin, northwestern Argentina: Journal of Sedimentary Research, v. 90, no. 2, p. 250–267. [Also available at https://doi.org/10.2110/jsr.2020.13.]

Mu, H., Yan, D.-P., Qiu, L., Yang, W.-X., Kong, R.-Y., Gong, L.-X., and Li, S., 2019, Formation of the Late Triassic western Sichuan foreland basin of the Qinling Orogenic Belt, SW China—Sedimentary and geochronological constraints from the Xujiahe Formation: Journal of Asian Earth Sciences, v. 183, 20 p.

Schenk, C.J., Mercier, T.J., Woodall, C.A., Finn, T.M., Le, P.A., Marra, K.R., Leathers–Miller, H.M., and Drake, R.M., II, 2020, Assessment of undiscovered conventional oil and gas resources of Southeast Asia, 2020: U.S. Geological Survey Fact Sheet 2020–3046, 2 p. [Also available at https://doi.org/10.3133/fs20203046.]

Shi, H., Shi, X., Glasmacher, U.A., Yang, X., and Stockli, D.F., 2016, The evolution of the eastern Sichuan Basin, Yangtze block since Cretaceous—Constraints from low temperature thermochronology: Journal of Asian Earth Sciences, v. 116, p. 208–221. [Also available at https://doi.org/10.1016/j.jseaes.2015.11.008.]

Wang, P.-J., Mattern, F., Didenko, N.A., Zhu, D.-F., Singer, B., and Sun, X.-M., 2016, Tectonics and cycle system of the Cretaceous Songliao Basin—An inverted active continental margin basin: Earth-Science Reviews, v. 159, p. 82–102. [Also available at https://doi.org/10.1016/j.earscirev.2016.05.004.]

Wang, T., Jin, Z., Shi, Z., Dai, X., and Cheng, R., 2019, Phanerozoic plate history and structural evolution of the Tarim Basin, northwestern China: International Geology Review, v. 62, no. 12, p. 1555–1569. [Also available at https://doi.org/10.1080/00206814.2019.1661038.]

Yang, C., Sun, J., Yang, Y., Yang, C., and Wang, J., 2020, Key factors controlling Mesozoic hydrocarbon accumulation in the southern East China Sea Basin: Marine and Petroleum Geology, v. 118, 20 p.

Yang, Y., Li, W., and Ma, L., 2005, Tectonic and stratigraphic controls on hydrocarbon systems in the Ordos Basin–A multicycle cratonic basin in central China: American Association of Petroleum Geologists Bulletin, v. 89, no. 2, p. 255–269. [Also available at https://doi.org/10.1306/10070404027.]

Zhao, S., Li, S., Liu, X., Suo, Y., Dai, L., Lou, D., Sun, W., Li, T., Wang, X., and Yang, Z., 2014, Intracontinental orogenic transition—Insights from structures of the east Junggar Basin between the Altay and Tianshan orogens: Journal of Asian Earth Sciences, v. 88, p. 137–148. [Also available at https://doi.org/10.1016/j.jseaes.2014.03.008.]

Zheng, Y.-F., Xiao, W.-J., and Zhao, G., 2013, Introduction to tectonics of China: Gondwana Research, v. 23, no. 4, p. 1189–1206. [Also available at https://doi.org/10.1016/j.gr.2012.10.001.]

Zhou, J.-B., Wilde, S.A., Zhao, G.-C., and Han, J., 2018, Nature and assembly of microcontinental blocks within the Paleo–Asian ocean: Earth-Science Reviews, v. 186, p. 76–93. [Also available at https://doi.org/10.1016/j.earscirev.2017.01.012.]

For More Information

Assessment results are also available at the USGS Energy Resources Program website, https://www.usgs.gov/energy-and-minerals/energy-resources-program.

China Assessment Team

Christopher J. Schenk, Tracey J. Mercier, Cheryl A. Woodall, Geoffrey S. Ellis, Thomas M. Finn, Phuong A. Le, Kristen R. Marra, Heidi M. Leathers-Miller, and Ronald M. Drake II.

ISSN 2327-6932 (online)
https://doi.org/10.3133/fs20213051